Two Dimension ZIF-derived Ultra-thin Cu-N/C Nanosheets as High-Performance Oxygen Reduction Electrocatalysts for High-Performance Zn-Air Batteries

Yi Guan, Nan Li, Yongliang Li, Lingna Sun, Yuan Gao*, Qianling Zhang, Chuanxin He, Jianhong Liu,Xiangzhong Ren**

Department of College of Chemistry and Environmental Engineering, Shenzhen University, Shenzhen, Guangdong 518060, P.R. China

*Corresponding author.

E-mail address: renxz@szu.edu.cn; liyli@szu.edu.cn; szgaoy311@163.com

Synthesis of ZIF-PHS

Cu/Zn ZIF-UNS was synthesized as fellows: $Zn(Ac)_2$ and $Cu(NO_3)_2 \cdot 3H_2O$ were dissolved in 40 mL of deionized water with the molar ratios of Zn^{2+}/Co^{2+} = 2:1, denoted as solution A. The 2-mIm and PVP was added to the same amount of deionized water denoted as solution B. Solution A and solution B are mixed and placed in a 60 ° water bath for 3 h with vigorously stirring. The reacted solution was then stirred at room temperature for 12 h. The detailed amount of metal salt and the corresponding ZIF-UNS products are listed in Table S1. The product was collected by

repeated centrifugation (8000 rpm, 15 min) and washed with deionized water for 4 times, and then dried in an oven at 60 °C overnight.

Table S1. The relationship diagram of the amounts of metal salt and the obtained products.

$Cu(NO_3)_2 \cdot 3H_2O$(mmol)	$Zn(Ac)_2$(mmol)	2-mIm(mmol)	PVP(g)	The product
2	4	16	0.5	Cu-N-UNS-1:2
3	3	16	0.5	Cu-N-UNS-1:1
4	2	16	0.5	Cu-N-UNS-2:1
5	1	16	0.5	Cu-N-UNS-5:1

Synthesis of Cu/Zn ZIF-UNS-L

$Zn(Ac)_2$ and $Cu(NO_3)_2 \cdot 3H_2O$ were dissolved in 40 mL of deionized water with the molar ratios of Zn^{2+}/Co^{2+} = 2:1, denoted as solution A. The 2-mIm and PVP was added to the same amount of deionized water denoted as solution B. Solution A and solution B are mixed and stirred at room temperature for 15 h. The product was collected by repeated centrifugation (8000 rpm, 15 min) and washed with deionized water for 4 times, and then dried in an oven at 60 °C overnight.

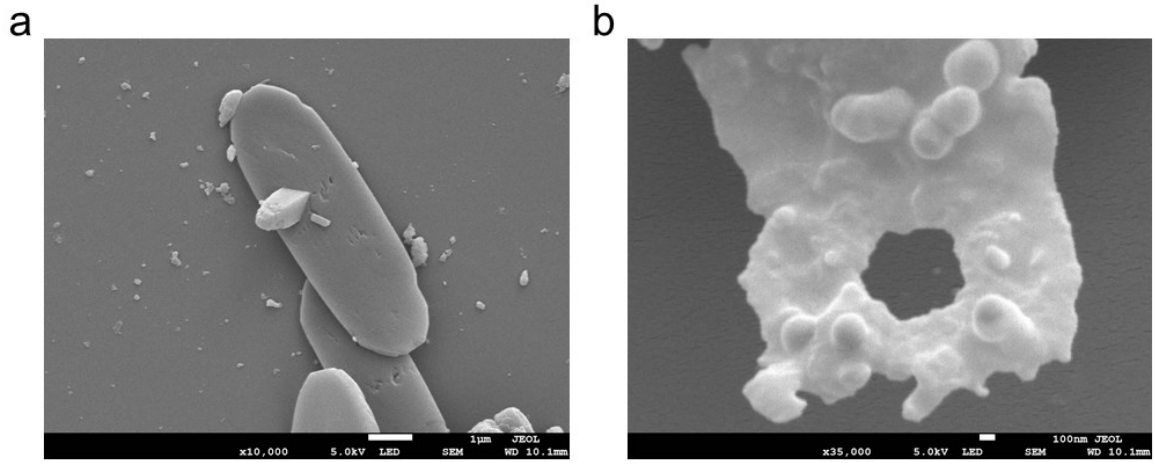

Fig. S1. SEM images of the (a) Cu/Zn ZIF-UNS-L and its product Cu/N-UNS (b).

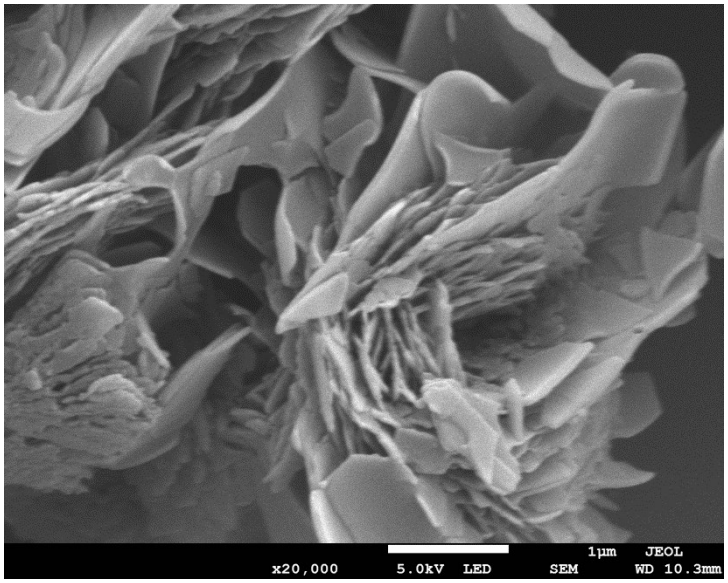

Fig. S2. SEM image of Cu/Zn ZIF-UNS after 3 hours water bath

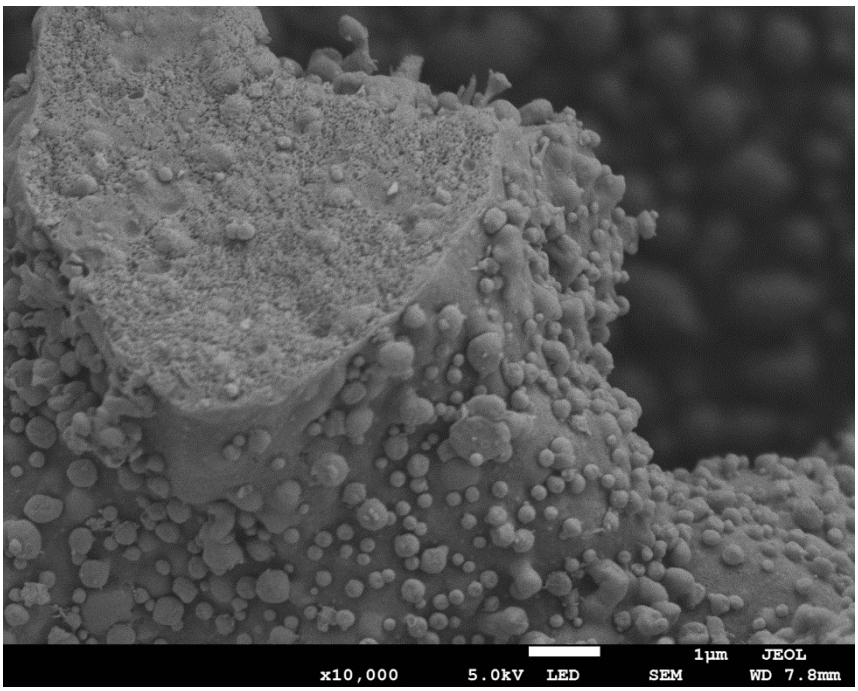

Fig. S3. SEM image of Cu-N-UNS-5:1.

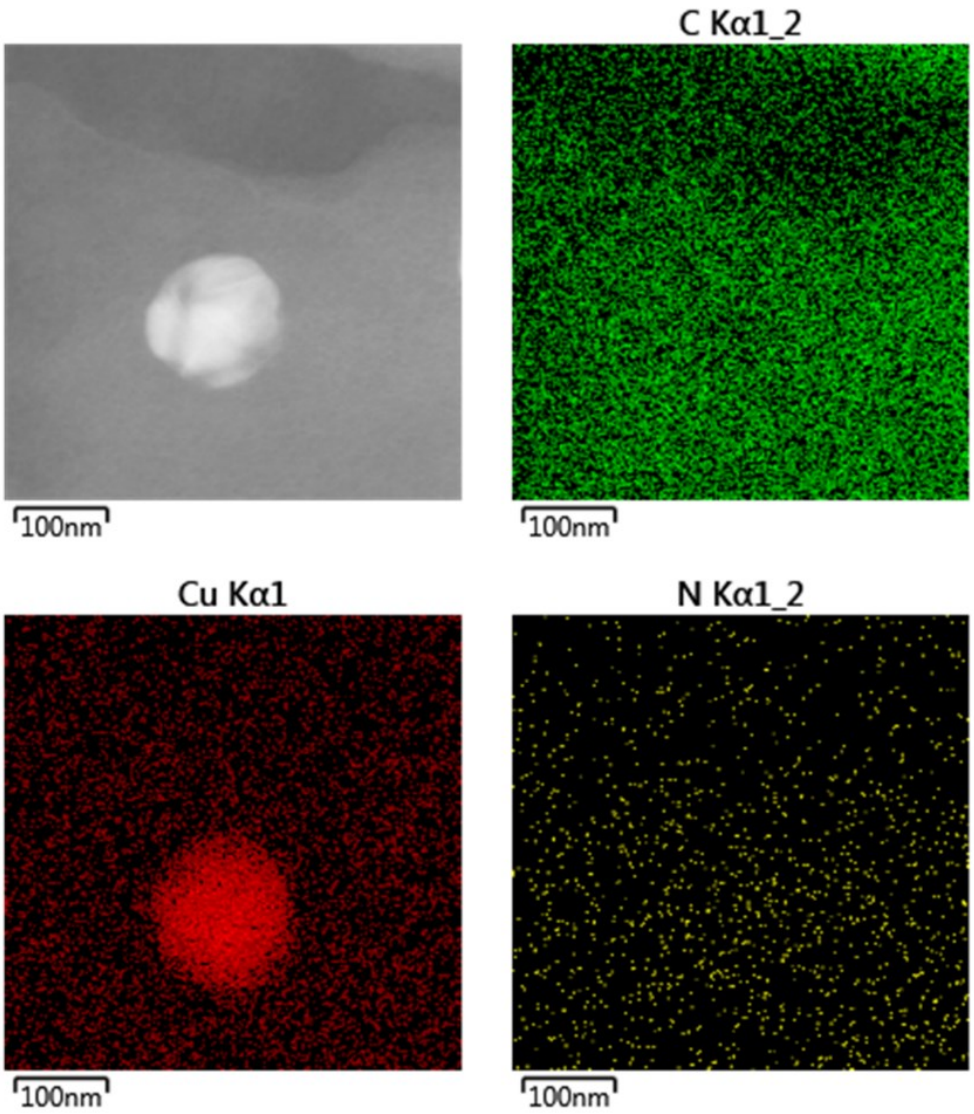

Fig. S4. TEM image and EDS mapping of Cu-N-UNS-2:1 showing Cu nanoparticles evenly distributed in the ultra-thin carbon micro-sheets.

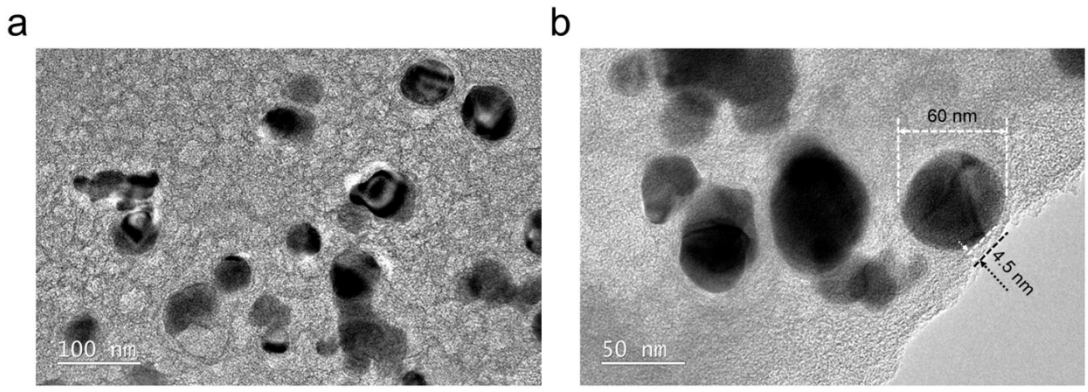

Fig. S5. TEM images of Cu-N-UNS-1:1.

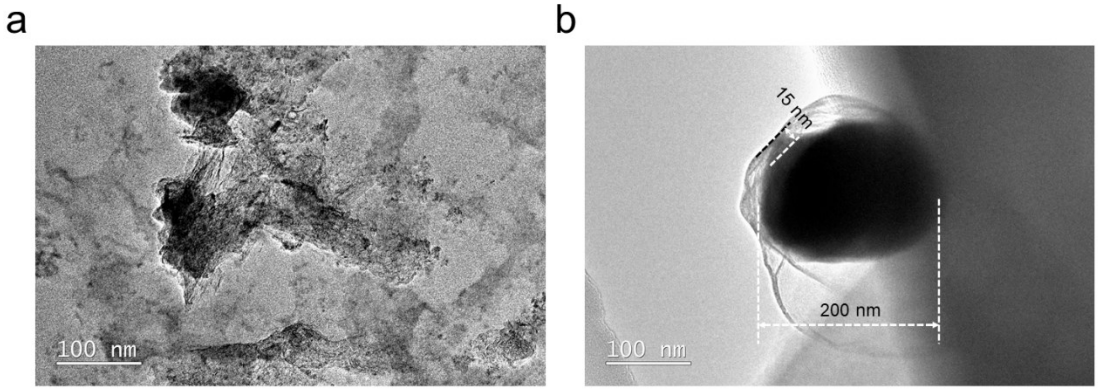

Fig. S6. TEM images of Cu-N-UNS-1:2.

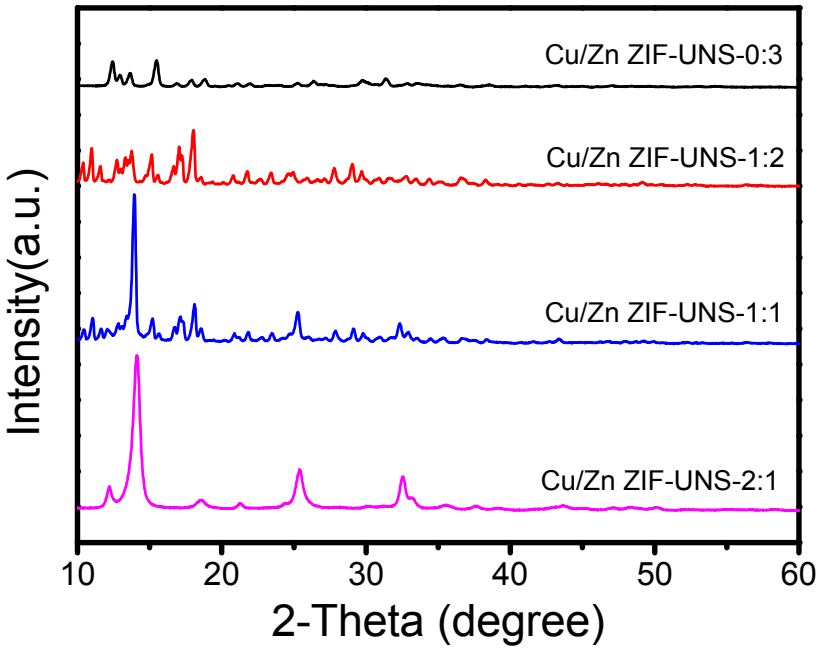

Fig. S7. XRD patterns of Cu/Zn ZIF-UNS samples.

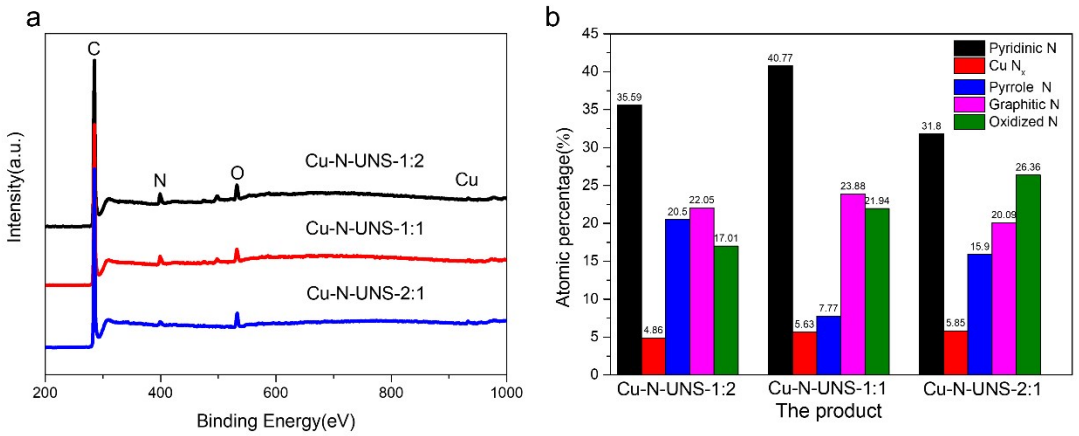

Fig. S8. XPS spectra (a) of different products derived from various precursors; and elemental composition (b) (atomic percentage) obtained from XPS analysis.

Table S2. Atomic ratios of Cu:N:C of the catalysts obtained from XPS analysis

Catalyst	Atomic %			
	Cu	C	N	O
Cu-N-UNS-1:2	0.14	89.5	5.8	4.56
Cu-N-UNS-1:1	0.17	90.2	5.2	4.43
Cu-N-UNS-2:1	0.2	92.4	4.8	2.6

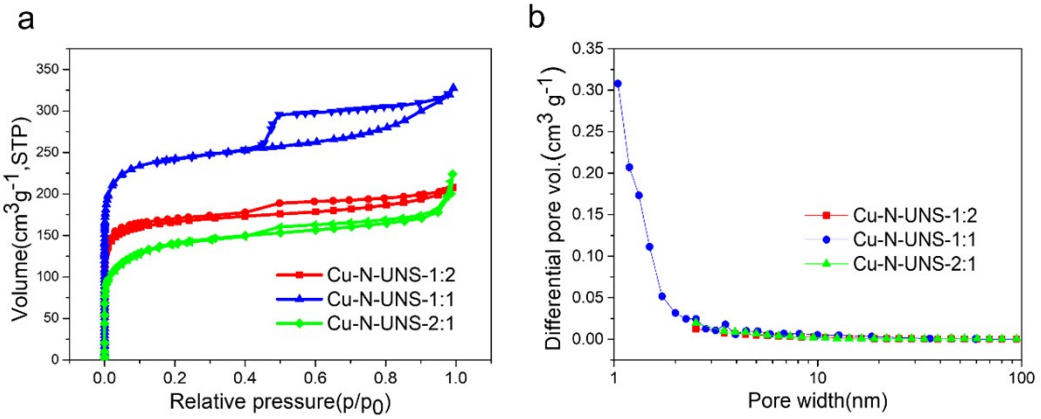

Fig. S9. (a) N_2 adsorption/desorption isotherms and (b) pore size distributions.

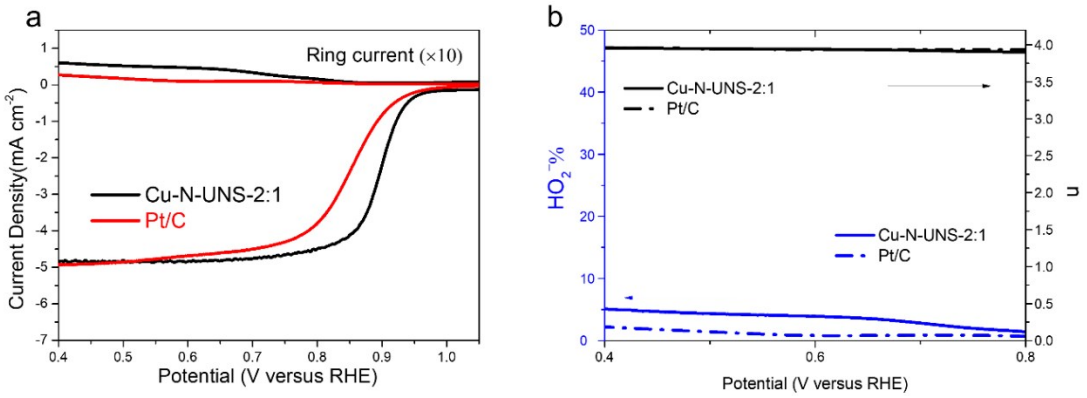

Fig. S10. The high diffusion-limited current densities and low ring current densities (×10) of Cu-N-UNS-2:1 and Pt/C (a). Percentage of peroxide in the total oxygen reduction products and the number of electron transfer (b) at the Cu-N-UNS-2:1 and Pt/C electrodes based on the RRDE result.

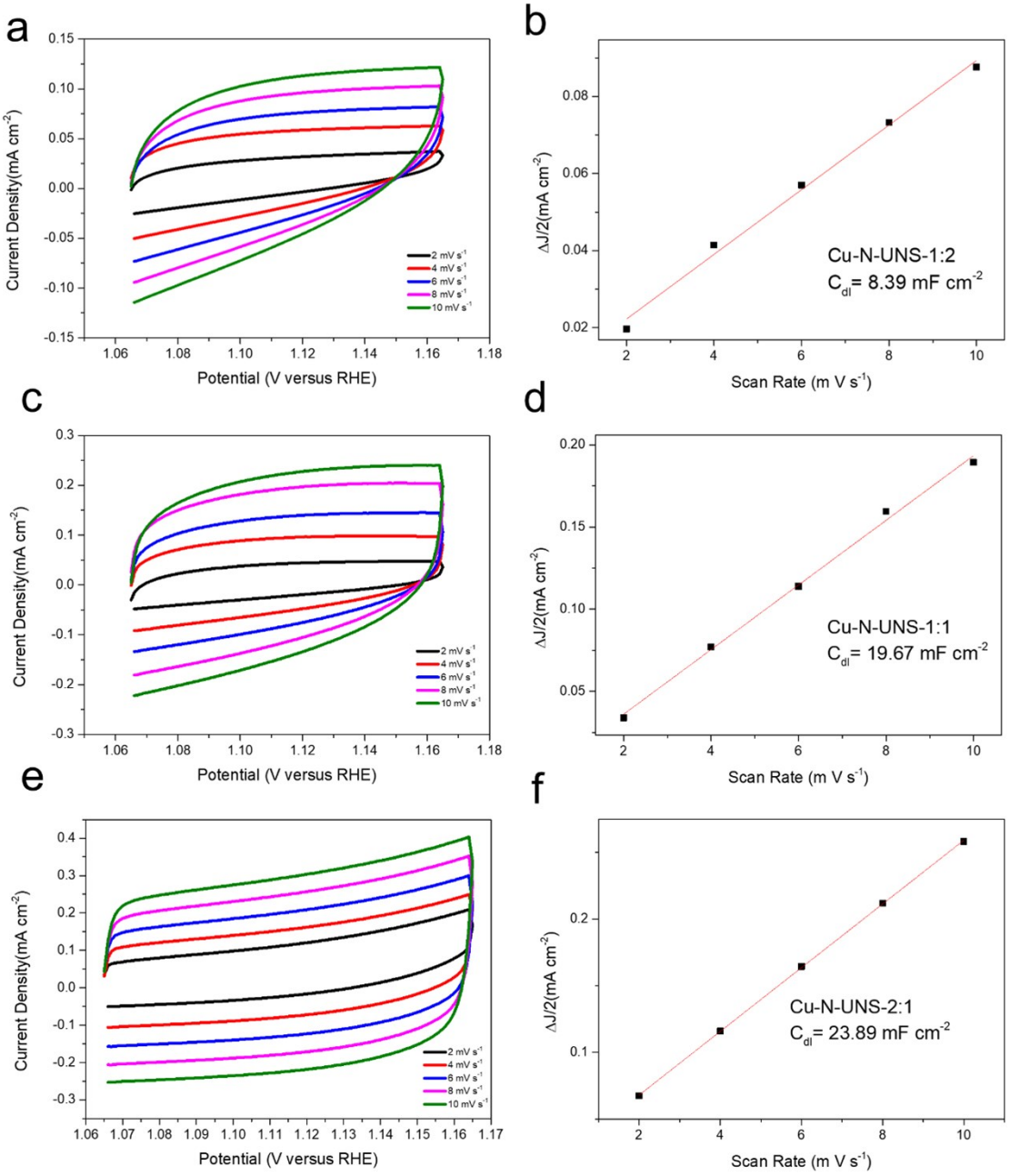

Fig. S11. Cyclic voltammograms in the region of 1.065-1.165 V vs. RHE at various scan rates and the corresponding linear fitting of the capacitive currents vs. scan rates to estimate the C_{dl}. (a) and (b) for Cu-N-UNS-1:2; (c) and (d) for Cu-N-UNS-1:1; (e) and (f) for Cu-N-UNS-2:1; (g) and (h) for Cu/N-UNS; (i) and (j) for Pt/C and the calculated C_{dl} values are shown in the insets.

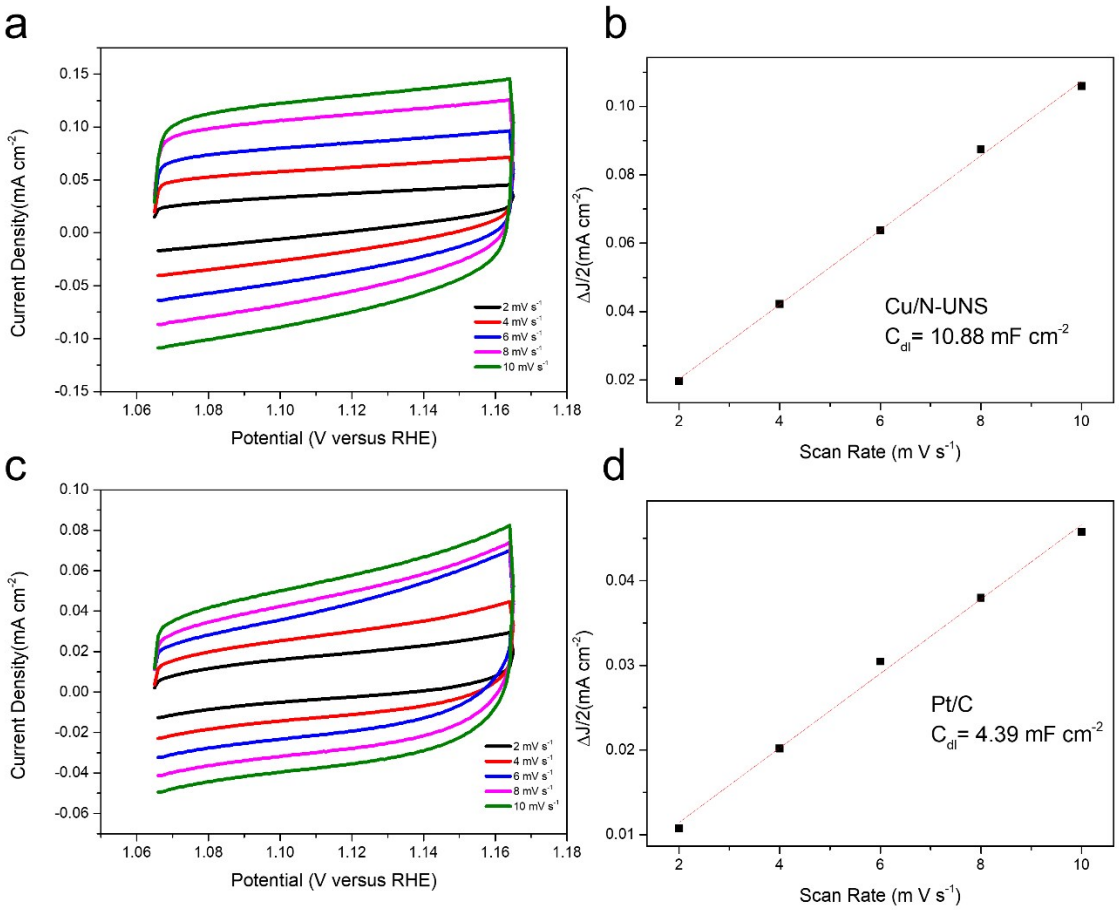

Fig. S12. Cyclic voltammograms in the region of 1.065-1.135 V vs. RHE at various scan rates and the corresponding linear fitting of the capacitive currents vs. scan rates to estimate the C_{dl}. (a) and (b) for Cu/N-UNS; (c) and (d) for Pt/C and the calculated C_{dl} values are shown in the insets.

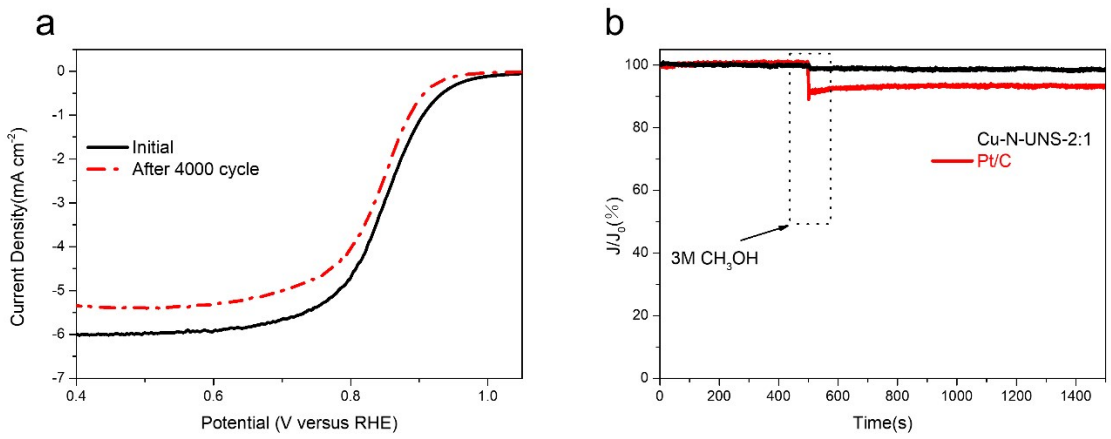

Fig. S13. (a) Pt/C before and after 4000 potential cycles at a potential range of 1.2–1.8 V versus RHE and a sweep speed of 100 mV s^{-1}; (b) Chronoamperometric response at 0.8 V after the introduction of 3M methanol into 65 ml of 0.1 M KOH solution for Cu-N-UNS-2:1 and Pt/C, respectively.

Table S3. Activities for ORR of as-prepared catalysts and Pt/C

Catalyst	E_{onset}(V)	$E_{1/2}$(V)	$J_{k\ at\ 0.85V}$(mA cm^{-2})
Cu-N-UNS-1:2	0.92	0.792	0.09544
Cu-N-UNS-1:1	0.921	0.81	1.023
Cu-N-UNS-2:1	0.987	0.898	28.86
Cu/N-UNS	0.92	0.811	0.924
Pt/C	1.003	0.85	5.04

Table S4. A survey of the catalytic performances of various ORR electrocatalysts from recent literatures.

Literature	Catalyst	ORR	
		E_{onset} (V vs. RHE)	$E_{1/2}$ (V vs. RHE)
This work	**Cu-N-UNS-2:1**	**0.987**	**0.898**
ACS Nano, 2019, DOI: 10.1021/acsnano.8b08692.	Cu−N−C	/	0.84
Nature Catalysis, 2018, 1, 781–786.	Cu SAs/N-C	/	0.895
Small, 2017, 13, 1700740.	25% Cu-N/C	0.914	0.813
Adv. Energy Mater. 2018, 1802263	$CoIn_2S_4$/S-rGO	0.93	0.82
ACS Appl Mater Interfaces, 2016, 8, 21431-21439.	Cu−N−C	/	−0.156 V vs (SCE)
Adv. Energy Mater. 2018, 8, 1701642	CoS_x@PCN/rGO	0.89	0.78
J. Mater. Chem. A, 2019, DOI: 10.1039/c9ta01953g.	Fe-N-C-800	/	0.883
Adv. Energy Mater. 2018, 1801495	rGO/CB_2/Co-Bi	0.88	0.7
Adv. Energy Mater.	DN-CP@G	N/A	0.801

2018, 1703539			
Adv. Mater. 2016, 28, 3000–3006	NCNF-1000	0.97	0.82
Adv. Energy Mater. 2017, 7, 1602420	N-GCNT/FeCo-3	1.03	0.92

Table S5. A survey of the performance of primary Zn-air batteries with various electrocatalysts

Literature	Catalysts	Loading (mg cm^{-2})	Peak power density (mW cm^{-2})
This work	**Cu-N-UNS-2:1**	**1**	**134.7**
Small, 2017, 13, 1700740.	25% Cu-N/C	1	132
Adv. Funct. Mater. 2017, 1705048	Co-N-CNTs	1	101
J. Mater. Chem. A, 2019, DOI: 10.1039/c9ta01953g.	Fe-N-C-800	2	135.3
Adv. Energy Mater. 2018, 1802263	$CoIn_2S_4$/S-rGO	N/A	133
Adv. Energy Mater.,	FeCo@MNC	1	115

2017, 7, 1602420			
Adv. Energy Mater. 2017, 7, 1602420	N-GCNT/FeCo-3	2	89.3
Adv. Energy Mater. 2018, 1800480	CoNi@NCNT/NF	N/A	127
Adv. Mater. 2018, 1705431	C-MOF-C2-900	0.5	105